Colloid Polym Sci (2009) 287:443–454
DOI 10.1007/s00396-008-1987-7

ORIGINAL CONTRIBUTION

Drying dissipative patterns of aqueous solutions of simple electrolytes and their binary mixtures on a cover glass

Tsuneo Okubo · Akira Tsuchida · Hiroki Togawa

Received: 3 November 2008 / Revised: 30 November 2008 / Accepted: 10 December 2008 / Published online: 15 January 2009

Abstract The drying dissipative patterns of aqueous solutions of simple electrolytes, KCl, NaCl, $CaCl_2$, and $LaCl_3$, were observed on a cover glass. The macroscopic broad rings were formed at the outside edge of the drying film area, which shrunk from the initial solution area especially at low salt concentrations. The drying area and the broad ring size decreased as the salt concentration decreased. The microscopic block-like and dendritic cross-like patterns were observed for all the salts. Size of single crystals dried on a cover glass increased as salt concentration increased. The drying patterns of the binary mixtures of the salts were also observed. Size of the broad ring increased sharply by mixing. The microscopic patterns were, on the other hand, insensitive to the mixing.

Keywords Drying dissipative structure · Pattern formation · Simple electrolytes · Broad ring pattern · Cover glass

Introduction

In general, most structural patterns in nature are formed spontaneously via self-organization processes accompanied with the dissipation of free energy and in the nonequilibrium state. Among several factors in the free energy dissipation of solutions and suspensions, the gravitational and the Marangoni convections are very important. In order to understand the mechanisms of the dissipative self-organization of the simple model systems instead of the much complex nature itself, the authors have studied the *convectional*, *sedimentation*, and *drying* dissipative patterns of solutions and colloidal suspensions as systematically as possible.

Most famous *convectional* pattern is the *Benard cell*, the *hexagonal circulating* one [1, 2]. Another typical convectional pattern is the *spoke-like lines*, which were observed in the whole area of liquid surface and appeared in various substrates sometimes accompanied with the large number of small *cell convections* in the normal direction of the spoke lines. So far as the authors know, the spoke lines have been observed by Terada et al. [3–5], for the first time, for the membranes of Chinese black ink on water surface. Thus, the authors like to call the spoke patterns as *Terada cell*. The Terada cells were observed clearly for the Chinese black ink in a glass dish [6], 100% ethanol suspensions of colloidal silica spheres [7], coffee with cream [8], Miso-soup [9], and colloidal crystals of poly(methyl methacrylate) colloidal spheres [10, 11]. Recently, the whole growing processes of the convectional patterns observed were summarized as seven steps [8, 9]: (a) the irregular circulating lines appeared at random in their flow direction at the initial stage on the substrates including cover glass, watch glass, and glass dish, (b) global flow of the convection at the surface layers from the center toward outward edge of the substrate, (c) the distorted Benard cells formed at the liquid surface, (d) the reversed global flow of convection at the liquid surface at the middle stage, (e) the growing of the broad ring-like sedimentation structure, (f) growing of the spoke lines from the outside edge toward the central area at the liquid surface layers, and (g) the

T. Okubo (✉)
Institute for Colloidal Organization,
Hatoyama 3-1-112,
Uji, Kyoto 611-0012, Japan
e-mail: okubotsu@ybb.ne.jp

T. Okubo
Cooperative Research Center, Yamagata University,
Johnan 4-3-16,
Yonezawa 992-8510, Japan

A. Tsuchida · H. Togawa
Department of Applied Chemistry, Gifu University,
Yanagido 1-1,
Gifu 501-1193, Japan

formation of the clusters and further bundles of the spoke lines at the final stage of convection.

Sedimentation pattern was studied, for the first time, in our laboratory for the aqueous suspensions of colloidal silica spheres (183 nm to 1.2 mm in diameter) [12–17], size-fractionated bentonite particles [18], and green tea [19] in the course of drying the suspensions. The broad ring patterns were formed within several 10 min in suspension state by the inward convectional flow of water and the colloidal particles at the liquid surface layers. It was clarified that the sedimentary particles were suspended above the substrate by the electrical double layers and moved by the balancing of the external fields including upward (or outward) convectional flow and sedimentation of the colloidal particles. The sharpness of the broad rings was sensitive to the change in the room temperature and/or humidity [14]. The main cause for the broad ring formation is the convectional outward flow of water and colloidal particles along the cell wall at the lower layers of liquid at the different rates, where the rate of the latter one is slower than that of the former one (step (e) in the convection described above in convectional pattern section). Quite recently, it was clarified that the dynamic cluster-like and bundle-like sedimentation patterns formed cooperatively from the spoke line-like convectional structures [8, 11].

Drying dissipative patterns have been studied for suspensions and solutions including colloidal silica spheres, coffee, black tea and green tea [8, 19] (for authors' work, see [20, 21–29]), linear-type polyelectrolytes, polymers, ionic and nonionic detergents and gels mainly on a cover glass, a watch glass, and a glass dish [20]. Macroscopic broad rings were formed for most solutes. Generally speaking, at high solute concentrations, the broad rings were formed at the outside edge of the drying films irrespective of the substrates used. However, the broad rings moved inward and their size decreased as sphere size increased and/or solute concentration decreased. Furthermore, the round hill was formed in the central area for the

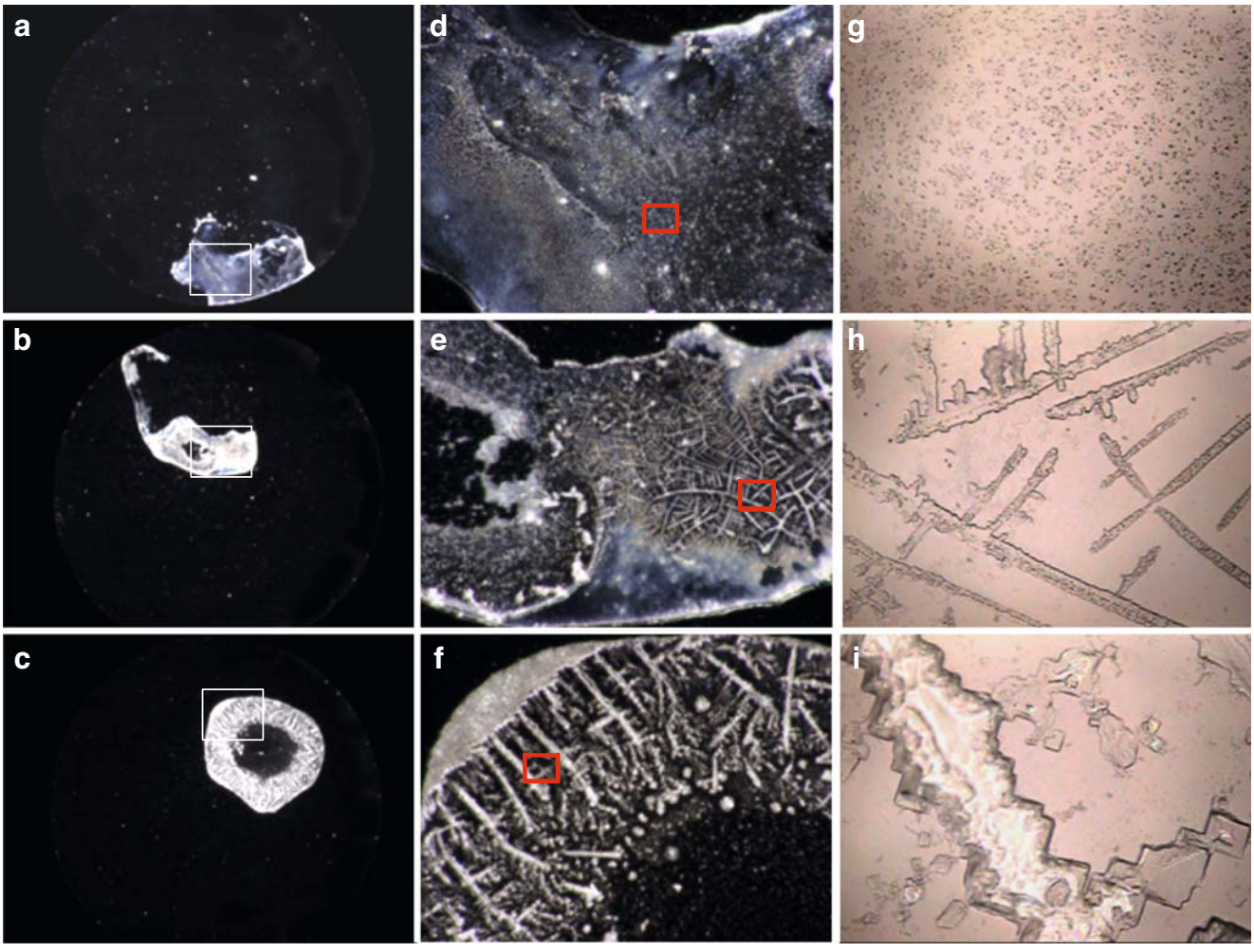

Fig. 1 Drying patterns of KCl solution on a cover glass at 25 °C. In water, 0.1 mL; H=38%; 1×10^{-5} (**a**, **d**, **g**), 1×10^{-4} (**b**, **e**, **h**), and 0.001 M (**c**, **f**, **i**); and length of the bar 1.0 mm (**a**–**c**), 200 μm (**d**–**f**), and 20 μm (**g**–**i**)

Table 1 Drying time (t) and broad ring size ratio (d_f/d_i) at the several experimental conditions

Electrolyte	Experimental conditions	Concentration (M)	t (min)	d_f/d_i
KCl	Open, 25 °C	1×10^{-6}	198	0.26
		1×10^{-5}	200	0.30
		1×10^{-4}	197	0.28
		0.001	208	0.35
		0.01	205	0.28
		0.1	191	0.37
KCl	Closed, 25 °C	1×10^{-6}	786	0.26
		1×10^{-5}	783	0.28
		1×10^{-4}	776	0.28
		0.001	768	0.32
		0.01	766	0.26
		0.1	762	0.36
KCl	Open, 40 °C	1×10^{-6}	59	0.32
		1×10^{-5}	62	0.39
		1×10^{-4}	60	0.42
		0.001	60	0.37
		0.01	67.5	0.41
		0.1	72.5	0.48
NaCl	Open, 25 °C	1×10^{-6}	198	0.23
		1×10^{-5}	207	0.23
		1×10^{-4}	202	0.21
		0.001	209	0.32
		0.01	196	0.39
		0.1	202	0.46
NaCl	Closed, 25 °C	1×10^{-6}	779	0.24
		1×10^{-5}	773	0.26
		1×10^{-4}	780	0.23
		0.001	768	0.33
		0.01	777	0.33
		0.1	758	0.40
NaCl	Open, 40 °C	1×10^{-6}	66	0.29
		1×10^{-5}	65.5	0.27
		1×10^{-4}	62.6	0.31
		0.001	61	0.44
		0.01	65.5	0.42
		0.1	60	0.56
$CaCl_2$	Open, 25 °C	1×10^{-6}	203	0.29
		1×10^{-5}	200	0.32
		1×10^{-4}	200	0.39
		0.001	214	0.39
		0.01	–	0.38
		0.1	–	0.49
$CaCl_2$	Closed, 25 °C	1×10^{-6}	759	0.34
		1×10^{-5}	763	0.41
		1×10^{-4}	767	0.41
		0.001	782	0.31
		0.01	–	0.32
		0.1	–	0.49
$CaCl_2$	Open, 40 °C	1×10^{-6}	69.5	0.5
		1×10^{-5}	68.5	0.7
		1×10^{-4}	65.5	0.6
		0.001	65.5	0.8
$LaCl_3$	Open, 25 °C	1×10^{-6}	203	0.21
		1×10^{-5}	207	0.21
		1×10^{-4}	200	0.53
$LaCl_3$	Closed, 25 °C	1×10^{-6}	66	0.32
		1×10^{-5}	70	0.40
		1×10^{-4}	69	0.74
$LaCl_3$	Open, 40 °C	1×10^{-6}	66	0.37
		1×10^{-5}	70	0.54
		1×10^{-4}	69	1

Humidity=38% (at 25 °C), unknown (at 40 °C)

nonspherical particles [18]. It should be mentioned that the pinning effect of the contact line of the drying drop proposed by Deegan et al. [30, 31] is not supported experimentally except special experimental conditions, at high solute concentrations, for example. Furthermore, agreement between the experiments and theories is not always successful yet. Main cause will be due to the insufficient experimental studies so far. Macroscopic spoke-like cracks or fine hills including flickering spokes were also observed for many solutes. Furthermore, beautiful patterns such as earth worm-like, branch-like, arc-like, block-like, star-like, cross-like, and string-like structures were observed in the microscopic scale. These microscopic drying patterns were often reflected from the shape, size, and/or flexibility of the solutes themselves. One of the very important findings in our experimental studies is that the primitive and vague sedimentation patterns were formed already in the liquid phase before dryness, and they grew toward fine structures in the processes of solidification [18].

In this work, drying dissipative patterns of aqueous solutions of simple electrolytes, KCl, NaCl, $CaCl_2$, and $LaCl_3$, were studied on a cover glass. Comparing the microscopic and macroscopic patterns of simple electrolytes with those other solutions and suspensions observed hitherto is the main purpose of this work. Clarification of the influences of the humidity, solute concentration on the structural patterns, and the broad ring size is also interesting.

Experimental

Materials

Potassium chloride (99.9% pure), sodium chloride solution, 0.1 M of standard aqueous solution, calcium chloride dihydrate (99.9%), and lanthanum (III) chloride heptahydrate (99.9%) were purchased from Wako Pure Chemicals Inc. (Osaka, Japan). These salts were used without further purification. Water used for the sample preparation was purified by a Milli-Q reagent grade system (Milli-RO5 plus and Milli-Q plus, Millipore, Bedford, MA, USA).

Observation of the dissipative structures

An amount of 0.1 mL of the aqueous salt solutions were dropped carefully and gently on a microcover glass (30× 30 mm, thickness no. 1, 0.12 to 0.17 mm, Matsunami Glass Co., Kishiwada, Osaka, Japan) in a plastic dish (52 mm in diameter, 10 mm in depth, type NH-52, As One Co., Tokyo, Japan). The cover glasses were used without further rinse. A pipette (1 mL, disposable serological pipette, Corning Lab. Sci. Co.) was used for the liquid dropping. Observation of the drying patterns was made for the solutions set on a desk until dried up completely in a room air-conditioned at 25 °C in most experiments. For the observation at 40 °C, the cover glass was set on a Sharmal Hotplate (type HHP-401, Iuchi Seiei Dou Co., Tokyo, Japan). The humidity of the room air of the laboratory was regulated between 38 and 61%. Concentrations of KCl, NaCl, $CaCl_2$, and $LaCl_3$ ranged from 1×10^{-6} to 0.1 M.

Macroscopic dissipative structures were observed on a Digital HD Microscope (type VH-7000, Keyence Co., Osaka, Japan). In order to check the reproducibility of the data, the macroscopic patterns of sodium chloride were observed again 5 years later from the original work on the simple electrolytes on a Canon EOS 10D digital camera with a macrolens (EF 50 mm, f=2.5) and a life-size converter EF. Drying processes with time were recorded on a video camera recorder (CCD-V188, Sony). Microscopic structures and the thickness profiles of the dried films were observed with a laser 3D profile microscope (type VK-8500, Keyence).

Results and discussion

Drying dissipative patterns of KCl

Figure 1 shows the drying patterns of KCl solutions in the macroscopic and microscopic scales at concentrations of 1×10^{-5}, 1×10^{-4}, and 0.001 M. Several important findings should be noted here. Firstly, (a) the drying area was localized at the corner of the outside area of the initial

Table 2 Effect of humidity on the drying time (t) and broad ring size ratio (d_f/d_i)

Electrolyte	H (%)	t (min)	d_f/d_i
KCl	38	208	0.35
	47	221	0.30
	49	264	0.31
	53	289	0.26
	56	300	0.24
	61	355	0.28
NaCl	38	209	0.32
	47	205	0.27
	49	263	0.31
	53	283	0.24
	56	290	0.23
	61	343	0.20
$CaCl_2$	38	214	0.39
	47	218	0.37
	49	281	0.34
	53	310	0.34
	56	320	0.34
	61	377	0.35

[KCl] = [NaCl] = [$CaCl_2$] = 0.001 M, at 25 °C

liquid area or at the central area. In other words, the diameter when the final drying area was assumed to be circular, d_f was smaller than that of the initial liquid circle, d_i. The ratios, d_f/d_i values were compiled in Table 1 with the data of drying times (t) at various salt concentrations ranging from 1×10^{-6} to 0.1 M and at several experimental conditions, i.e., without cap at 25 °C, with cap at 25 °C, and without cap at 40 °C. The ratios were much smaller than unity and increased as salt concentration increased, though the experimental errors were rather large. These tendencies of the d_f/d_i values have been observed so often for the drying experiments of solutions and suspensions including colloidal silica spheres of CS45 (56.3 nm in diameter) [32], CS82 (103 nm) [33], and CS301 (311 nm) [32], polystyrene spheres [34], poly(methyl methacrylate) spheres [11, 35], coffee [8], ionic detergents [36], neutral and water-soluble detergents [37], biological polyelectrolytes (sodium poly-α-L-glutamate and poly-L-lysine hydrochloride [38], and polyethylene glycol (PEG) [39], for example. It should be mentioned that the d_f/d_i values were close to unity in many cases and quite insensitive to the high solute concentration. The shift of the drying area took place at the rather low solute concentrations. It should be noted further that the d_f/d_i values were also sensitive to other several experimental parameters in addition of the solute concentration. The d_f/d_i values of PEG solutions decreased significantly from unity as molecular weight of PEG decreased [39]. It is highly plausible that the main reason why the ratios of the simple salts are small from unity is due to the very low molecular weight of the simple salts. The d_f/d_i values of thermosensitive gel spheres of poly(*N*-isopropyl acrylamide) decreased sharply and transitionally at low

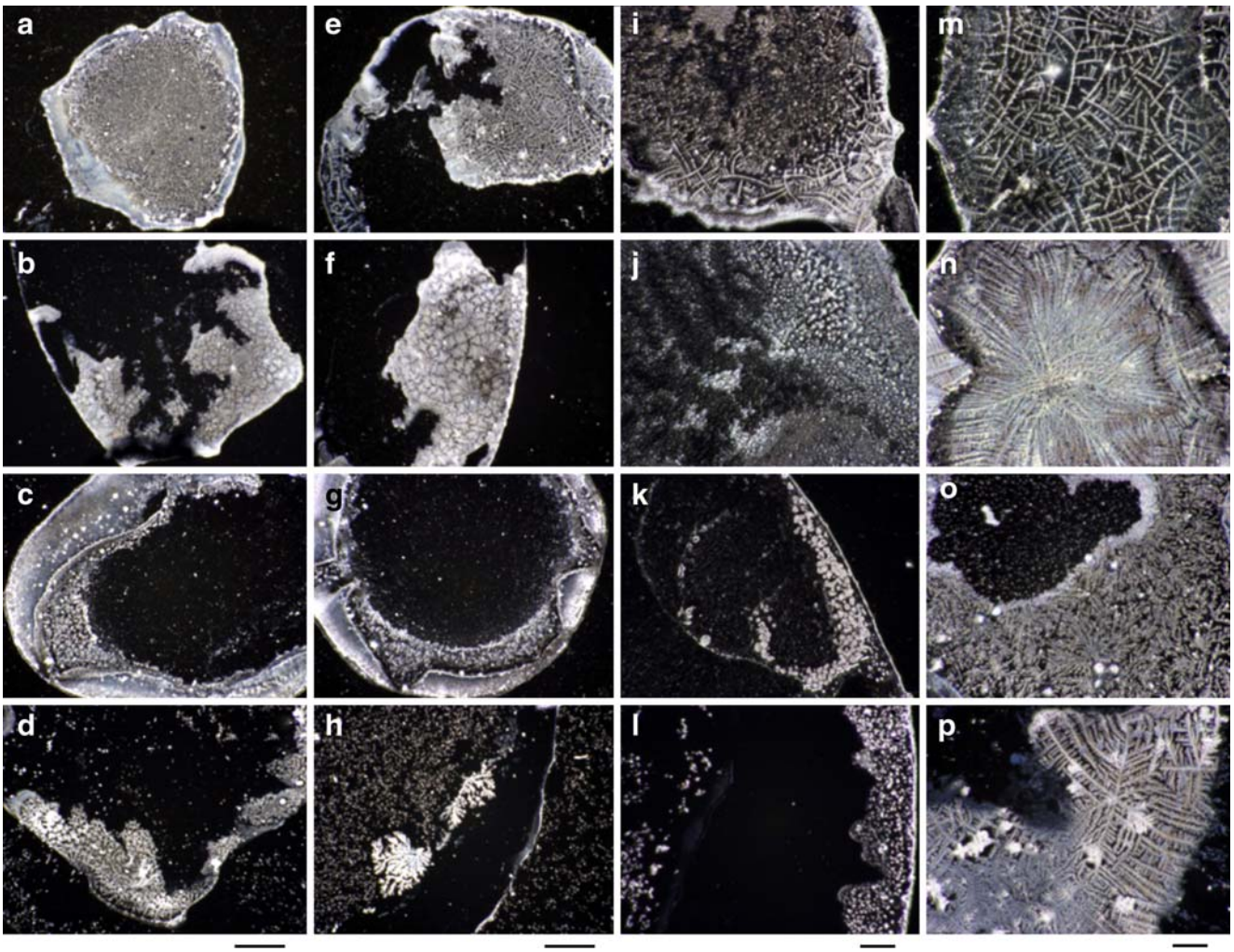

Fig. 2 Drying patterns of KCl (**a**, **e**, **i**, **m**), NaCl (**b**, **f**, **j**, **n**), $CaCl_2$ (**c**, **g**, **k**, **o**), and $LaCl_3$ (**d**, **h**, **l**, **p**) solutions on a cover glass at various experimental conditions. Salt=1×10^{-4} M, **a**–**d** T=25 °C, H=49%, and length of the bar=500 μm; **e**–**h** T=25 °C, H=61%, and length of the bar=500 μm; **i**–**l** T=40 °C, H=unknown, and length of the bar=200 μm; and **m**–**p** closed with cap, T=25 °C, H=unknown, and length of the bar=200 μm

temperatures [40]. The drying area shifted toward inner area of the dried film for the ethyl alcohol and/or ethyl alcohol plus methyl alcohol mixture suspensions of colloidal silica spheres on a cover glass [41]. In the binary and ternary mixtures of colloidal silica spheres, furthermore, the pattern area of larger spheres always appeared at the inner area of a dried film [16, 17].

Secondly, the broad rings were always observed at the outside edge of the dried area in the macroscopic scale. Thus, the d_f values are the same as broad ring size. The width of the broad ring increased sharply as the initial salt concentration increased (see Fig. 1a–c). A main cause for the broad ring formation is due to the convectional flow of water and KCl solutes in the different rates, where motion of salt solutes is slower than that of water molecules. Especially, the global outward convectional flow of water and solutes at the lower layers of liquid is important for the broad ring formation (see [20], for example).

Thirdly, the microscopic single crystals of KCl were observed in the extended pictures. Crystal size increased as initial salt concentration increased on a cover glass (Fig. 1g–i). This concentration dependency is opposite to the usual crystallization mechanism via the homogeneous nucleation in solution, where crystal size decrease as concentration increases. Important role of the wall of the substrate on the salt crystallization is highly plausible. Crystal structure of KCl is known as sodium chloride-type and the cubic lattice structures. Lattice constant is 629.3 pm at 25 °C. Shape of the single crystals changed from block-like to dendritic cross-like as KCl concentration increased. The reason, why number of nuclei increases with decreasing salt concentration on a cover glass, is not clear yet. Here, it is interesting to note that the information of the *salt concentration* in solution is *transferred* into the drying patterns of *crystal size and shape*.

Influence of the humidity on KCl crystallization is shown in Table 2. The d_f/d_i values decreased slightly as

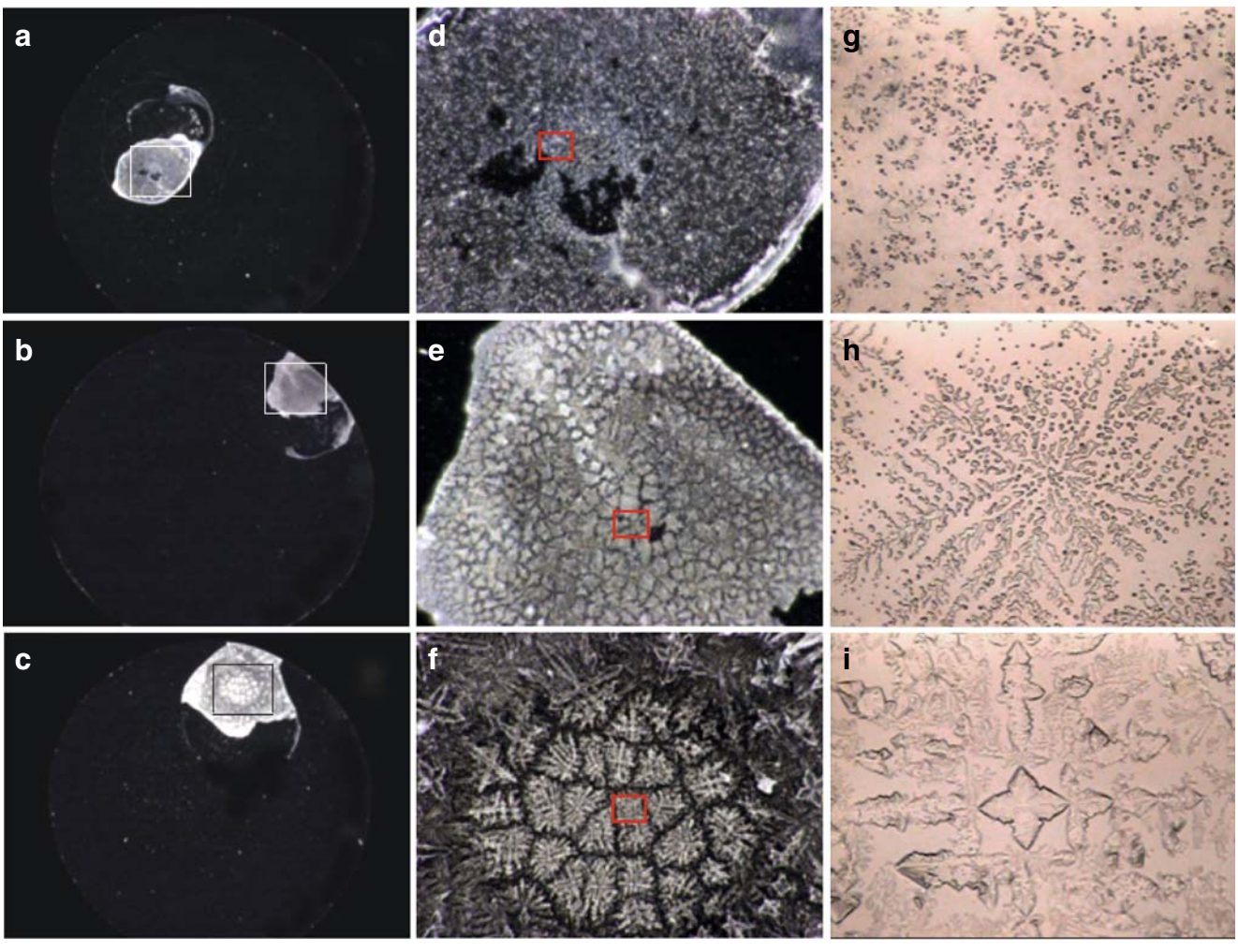

Fig. 3 Drying patterns of NaCl solution on a cover glass at 25 °C. In water, 0.1 mL; H=38%; 1×10^{-5} (**a**, **d**, **g**), 1×10^{-4} (**b**, **e**, **h**), and 0.001 M (**c**, **f**, **i**); and length of the bar=1.0 mm (**a**–**c**), 200 μm (**d**–**f**), and 20 μm (**g**–**i**)

the humidity increased, though the experimental errors of the ratios are rather large. Table 1 demonstrates that the d_f/d_i values of KCl in the open conditions are slightly larger than those in the closed. In the closed condition, the humidity should be much high compared with the open condition. Here, it should be further recalled that the broad rings of aqueous colloidal silica suspensions formed at the inner area in addition to the outside edge when the dryness proceeded at the high humidity atmosphere [42]. Thus, the high humidity accompanied with the long drying time is certainly favorable for the decrease of the d_f/d_i, though the reason is not always clear. The d_f/d_i values at 40 °C were clearly larger than those at 25 °C (compare the d_f/d_i values open at 25 °C and open at 40 °C). The reason for this temperature effect is also not clear yet. The drying time (t) increased as temperature and/or humidity decreased and/or increased, respectively. The t value was insensitive to the salt concentration (see Table 1).

The microscopic patterns of KCl at 1×10^{-4} M are shown in the top lines of Fig. 2a, e, i, m in the experimental conditions, H=49% at 25 °C, 61% at 25 °C, open at 40 °C, and closed at 25 °C, respectively. Humidity did not influence the microscopic structure of KCl (compare Figs. 1e and 2a, e). However, in the closed condition at 25 °C (Fig. 2m), cross-like patterns prevailed in the whole drying area. On the other hand, the microscopic structures at 40 °C were mainly block-like and the dendritic cross-like patterns were observed only around edge area (see Fig. 2i). These observations support that the very slow drying processes are favorable for the microscopic fine patterns.

Drying dissipative patterns of NaCl

Figure 3 shows the macroscopic and microscopic drying patterns of NaCl at salt concentrations of 1×10^{-5}, 1×10^{-4}, and 0.001 M at H=38% and at 25 °C. The quite similar

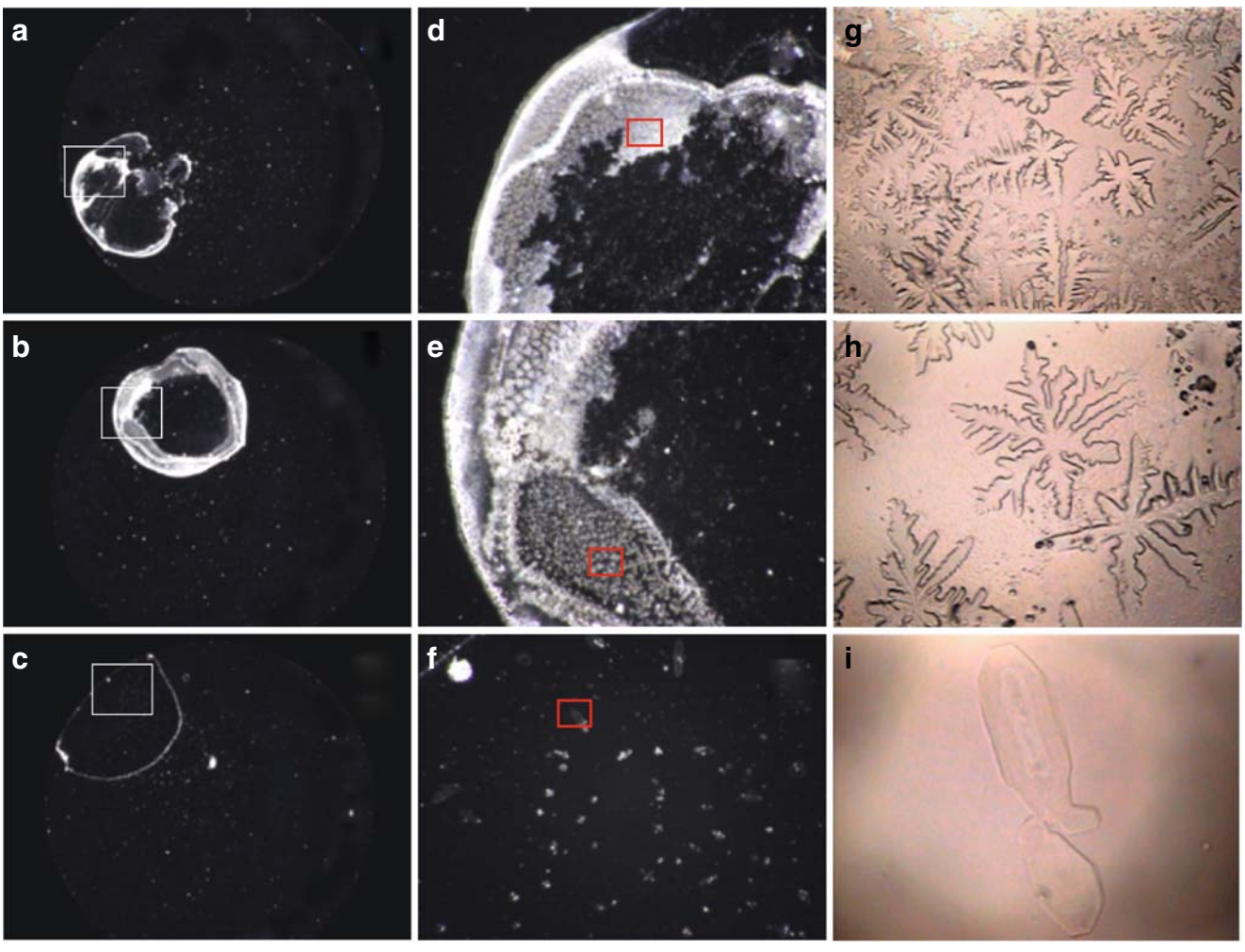

Fig. 4 Drying patterns of $CaCl_2$ solution on a cover glass at 25 °C. In water, 0.1 mL; H=38%; 1×10^{-5} (**a**, **d**, **g**), 1×10^{-4} (**b**, **e**, **h**), and 0.001 M (**c**, **f**, **i**); and length of the bar=1.0 mm (**a**–**c**), 200 μm (**d**–**f**), and 20 μm (**g**–**i**)

results as KCl were observed for d_f/d_i values. The ratios were also much smaller than unity and increased as salt concentration increased (see also Table 1). The broad rings were always observed at the outside edge of the shrunk dried area. Furthermore, size of the single crystals in the microscopic scale increased as initial salt concentration increased. The d_f/d_i values decreased as the humidity increased. These results of NaCl are similar to those of KCl. It should be mentioned here that the drying patterns of sodium chloride at the concentrations at 0.1, 0.3, and 1.0 M were observed 5 years later from the original work on the simple salts. The reproducibility of the patterns at 0.1 M was satisfactory. However, the drying patterns at 0.3 and 1.0 M, which were observed for the first time in the author's laboratory, were quite different from those at the lower concentrations than 0.1 M. The broad ring-like macroscopic patterns were not observed at 0.3 and 1.0 M. Instead, the central area was higher than the outer region. Furthermore, the shrunk film was composed of the giant size single crystals of sodium chloride and the small size of block-like patterns at the central and outer areas, respectively. Observation of the drying patterns is interesting in future. The microscopic structure of NaCl was insensitive to the humidity of the atmosphere. In the closed condition at 25 °C (see Fig. 2n), dendritic cross-like patterns prevailed in the whole drying area. On the other hand, the microscopic structures at 40 °C were mainly block-like just like KCl (see Fig. 2j, i). The crystal structures of NaCl and KCl are sodium chloride-type cubic lattices and quite similar to each other. The lattice spacing of NaCl is 564 pm. Furthermore, it should be noted that the solubilities in water are almost the same, 26.4 wt.% for both salts. The melting points, boiling points, and specific gravities differ slightly as 800 °C and 776 °C, 1,413 °C and 1,500 °C, and 2.164 g/cm^3 (at 20 °C) and 1.989 g/cm^3, respectively. Thus, quite similar drying

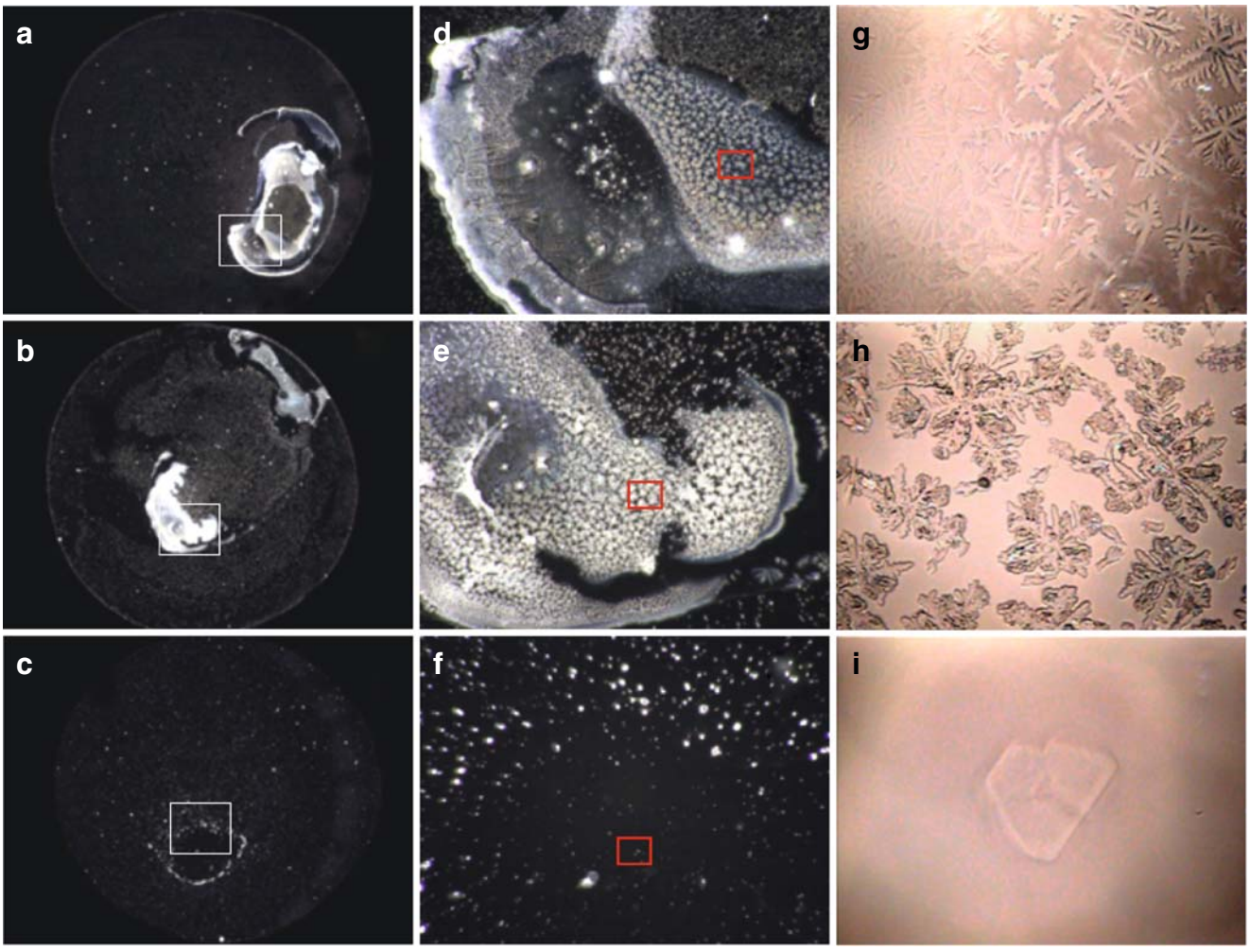

Fig. 5 Drying patterns of $LaCl_3$ solution on a cover glass at 25 °C. In water, 0.1 mL; H=38%; 1×10^{-5} (**a**, **d**, **g**), 1×10^{-4} (**b**, **e**, **h**), and 0.001 M (**c**, **f**, **i**); and length of the bar=1.0 mm (**a**–**c**), 200 μm (**d**–**f**), and 20 μm (**g**–**i**)

patterns between NaCl and KCl in macroscopic and microscopic scales are understandable from the similarity of the chemical structures and properties.

Drying dissipative patterns of $CaCl_2$

Figure 4 shows the macroscopic and microscopic drying patterns of $CaCl_2$ at the concentrations of 1×10^{-5}, 1×10^{-4}, and 0.001 M. The dendritic microscopic patterns of single crystals were observed (see the pictures shown in Fig. 4g, h), which are similar to those of KCl and NaCl. The crystal size increased as salt concentration increased. The broad rings were also observed at the outside edges of the shrunk drying area, which are again similar to those of KCl and NaCl. The d_f/d_i values looked to increase slightly as initial salt concentration increases. These results of $CaCl_2$ are also similar to those of

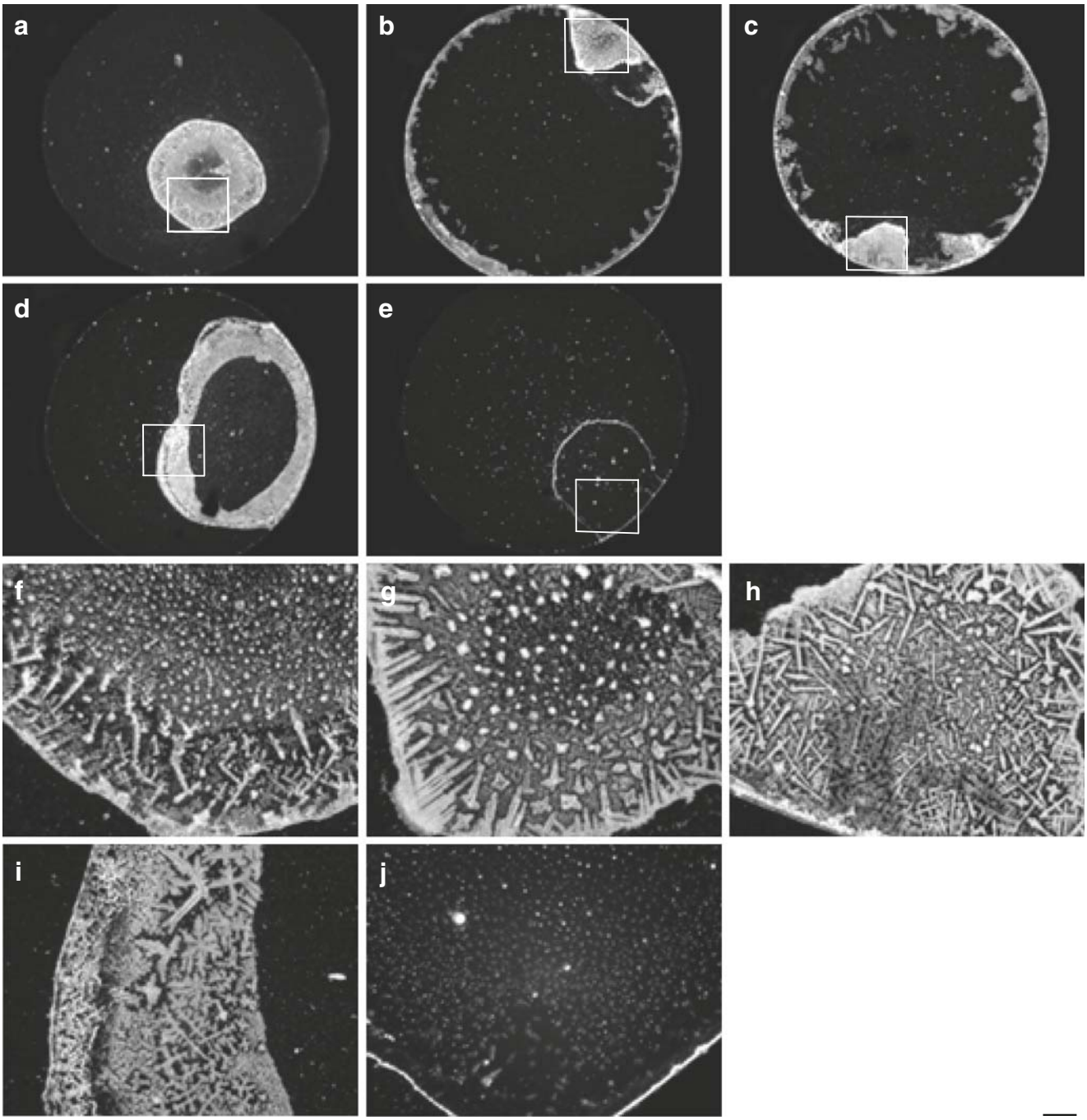

Fig. 6 Drying patterns of binary mixtures of KCl and $CaCl_2$ at 25 °C. H= 38%; **a**, **f** [KCl]=0.001 M, [$CaCl_2$]=0 M; **b**, **g** [KCl]=7.5×10^{-4} M, [$CaCl_2$]=2.5×10^{-4} M; **c**, **h** [KCl]=5×10^{-4} M, [$CaCl_2$]=5×10^{-4} M; **d**, **i** [KCl]=2.5×10^{-4} M, [$CaCl_2$]=7.5×10^{-4} M; **e**, **j** [KCl]=0 M, [$CaCl_2$]= 0.001 M; and length of the bar=1.4 mm (**a**–**e**) and 200 μm (**f**–**j**)

KCl and/or NaCl. The dried crystal structure at 25 °C is trigonal lattice of calcium hexahydrate, and its solubility in water is 45.3 wt.%. The melting and boiling temperatures and specific density are known to be 774 °C, 1,600 °C, and 2.15 g/cm^3 (15 °C), respectively. It is interesting to note that the quite similar patterns were observed among KCl, NaCl, and $CaCl_2$ in the macroscopic and microscopic scales.

Drying dissipative patterns of $LaCl_3$

Crystal structure of $LaCl_3$ is well known as hexagonal lattice and its solubility in water is 49.3 wt.%. Melting point and specific density of $LaCl_3$ solid are 852 °C and 3.84 g/cm^3, respectively. Figure 5 shows the macroscopic and microscopic drying patterns of $LaCl_3$ at the concentrations of 1×10^{-5}, 1×10^{-4}, and 0.001 M. The dendritic microscopic patterns of $LaCl_3$ were clearly observed especially at the low salt concentrations. The crystal size increased again as salt concentration increased. The shrunk ratios of the broad ring, d_f/d_i values, increased as salt concentration increased. Four pictures at the bottom line of Fig. 2 show that the microscopic structures of $LaCl_3$ are insensitive to the humidity. In the closed system at 25 °C, dendritic pattern formation was again enhanced. The microscopic structures at 40 °C were, on the other hand, mainly block-like, which is a similar tendency to KCl, NaCl, and $CaCl_2$.

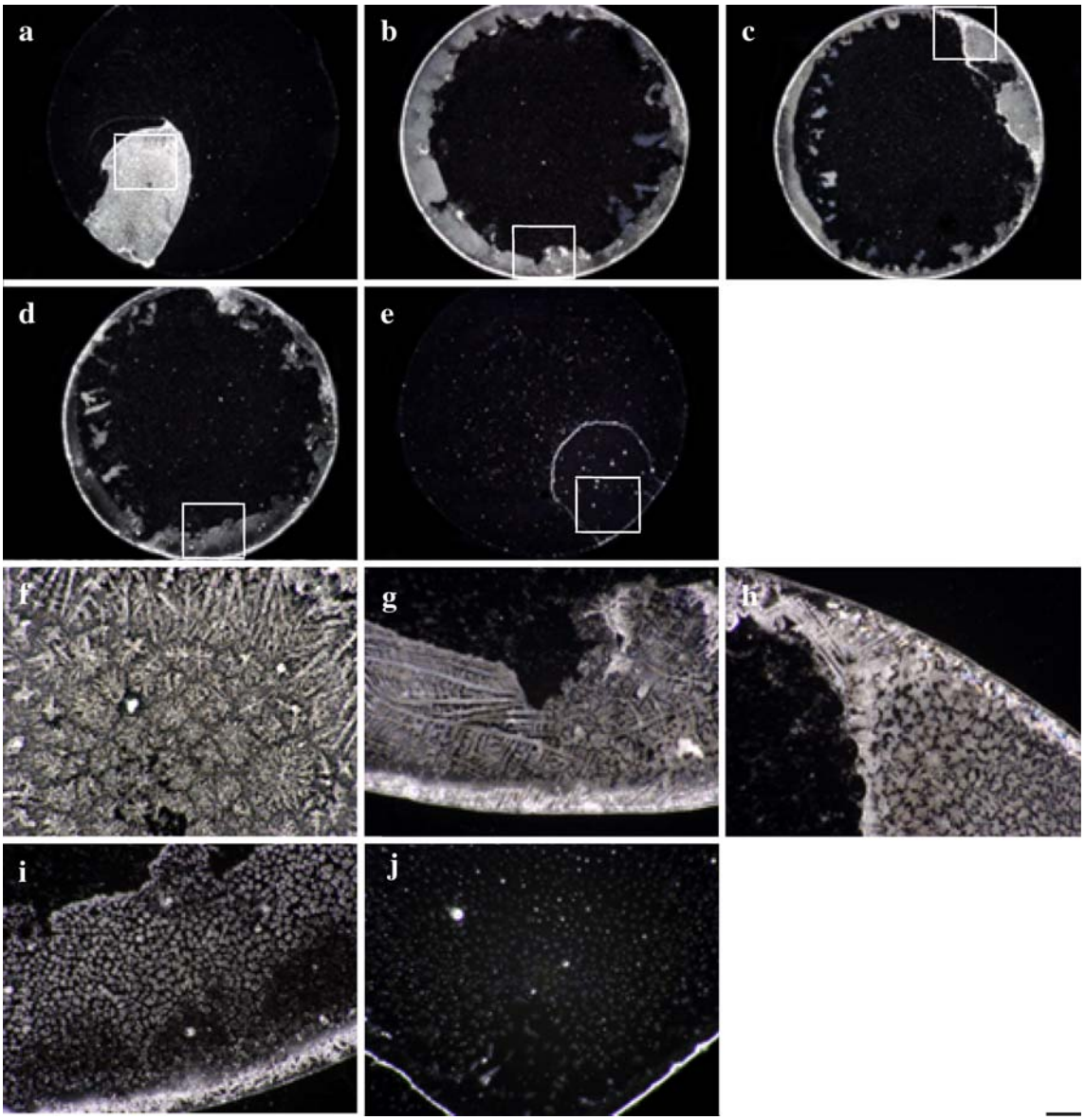

Fig. 7 Drying patterns of binary mixtures of NaCl and $CaCl_2$ at 25 °C. H=38%; **a**, **f** [NaCl]=0.001 M, [$CaCl_2$]=0 M; **b**, **g** [NaCl]=7.5×10^{-4} M, [$CaCl_2$]=2.5×10^{-4} M; **c**, **h** [NaCl]=5×10^{-4} M, [$CaCl_2$]=5×10^{-4} M; **d**, **i** [NaCl]=2.5×10^{-4} M, [$CaCl_2$]=7.5×10^{-4} M; **e**, **j** [NaCl]=0 M, [$CaCl_2$]=0.001 M; and length of the bar=1.4 mm (**a**–**e**) and 200 μm (**f**–**j**)

Here, comparing the d_f/d_i values of all the salts given in Tables 1 and 2, the ratios look to increase in the order,

$$KCl \cong NaCl < CaCl_2 < LaCl_3. \quad (1)$$

In other words, the d_f/d_i value increased as molecular weight and/or ionic valency of cations increased. This order agrees with that observed for poly(ethylene glycol) having various molecular weights. However, the authors do not know exactly why this order appeared. Surface tension of the initial solutions will be one of the most plausible causes to decide the d_f/d_i values of the dried film. The drying frontier of the liquid of higher surface tension will move easier toward central area. However, interactions between solutes and the cover glass will not be neglected. For simple electrolytes, for example, the electrostatic attraction between divalent and trivalent cations and the negatively charged glass wall intermediated with the electrical double layers formed along the cell wall will more or less retard the motion of these multivalent ions. Thus, it is highly plausible that the convectional flow of the salt ions in the lower layers of the liquid along the cell wall, which is one of the most important factors to make the broad ring, is influenced.

Drying dissipative patterns of the binary mixtures of simple salts

Figures 6 and 7 show the macroscopic (a to e) and microscopic drying patterns (f to j) of KCl + $CaCl_2$ and

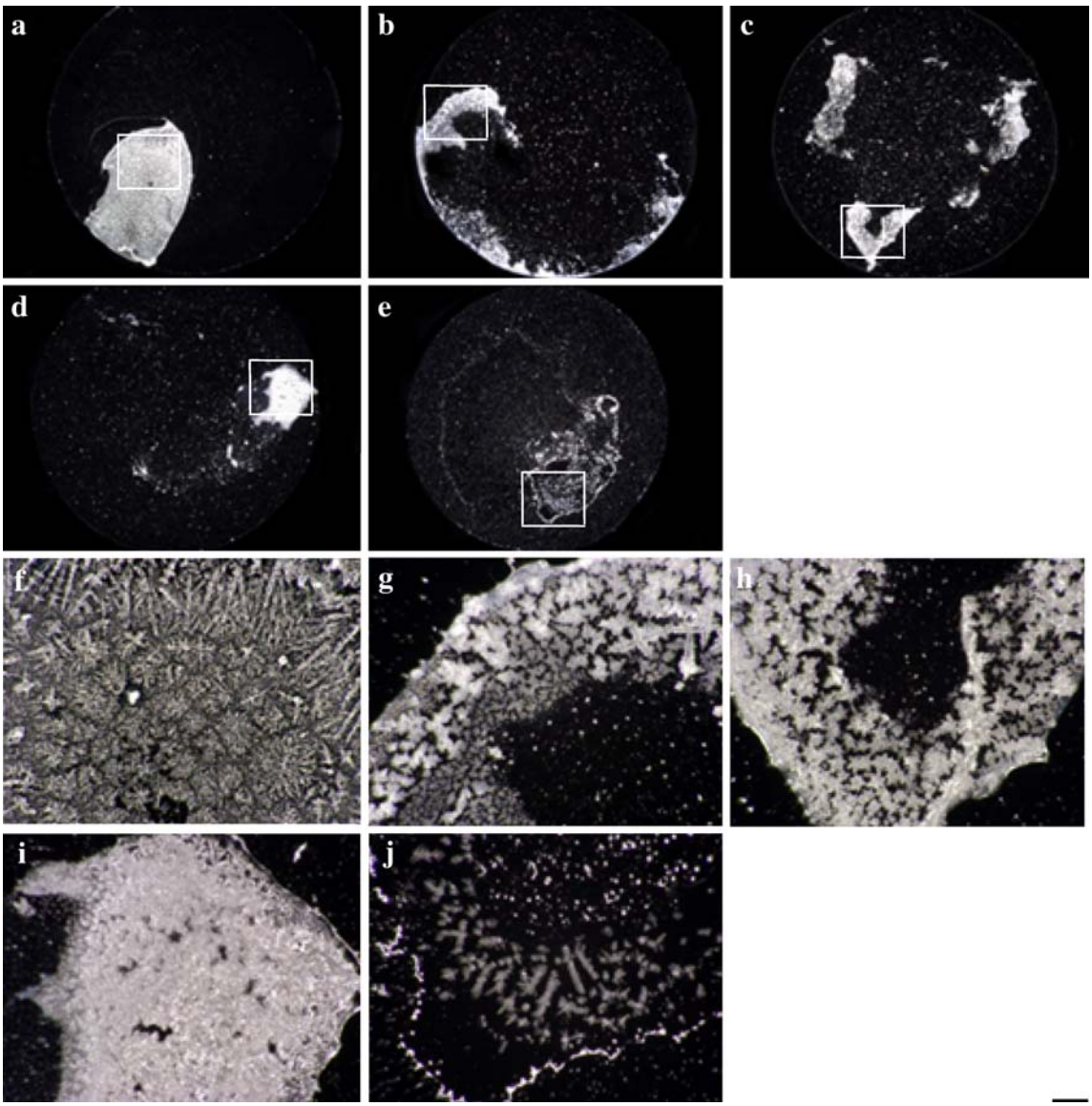

Fig. 8 Drying patterns of binary mixtures of NaCl and $LaCl_3$ at 25 °C. H=38%; **a**, **f** [NaCl]=0.001 M, [$LaCl_3$]=0 M; **b**, **g** [NaCl]=7.5×10^{-4} M, [$LaCl_3$]=2.5×10^{-4} M; **c**, **h** [NaCl]=5×10^{-4} M, [$LaCl_3$]=5×10^{-4} M; **d**, **i** [NaCl]=2.5×10^{-4} M, [$LaCl_3$]=7.5×10^{-4} M; **e**, **j** [NaCl]=0 M, [$LaCl_3$]=0.001 M; and length of the bar=1.4 mm (**a**–**e**) and 200 μm (**f**–**j**)

NaCl + $CaCl_2$ mixtures at different mixture ratios and at 0.001 M of total salt concentration. Interestingly, size of the broad rings increased sharply by the mixing the two components for both the mixtures. The microscopic structures were dendritic cross-like patterns and any differences were not observed by the mixing processes for the two mixtures. By the addition of one fourth of $LaCl_3$ to the NaCl solution (see Fig. 8b), the size of the broad ring increased transitionally. By further addition of $LaCl_3$, size of the broad ring increased and the d_f/d_i value reached unity for purely $LaCl_3$ (see Fig. 8e). The reason why the size of the broad ring increases by the binary mixing is not clear-cut. For the mixtures of KCl and NaCl, though the observation was not made in this work, the crystal structure of the mixtures should be similar to each single component systems, since the crystal structures and lattice constants of KCl and NaCl do not differ so much. Then, the formation of the substituted solid-type alloy structures is highly plausible even on the substrate. For the mixtures of KCl + $CaCl_2$, NaCl + $CaCl_2$ and NaCl + $LaCl_3$, the alloy crystals will not be so easily formed instead. The mixtures of the single crystals of each salt will be formed. These features will be correlated to the enlargement of the broad rings by mixing.

Concluding remarks

The drying dissipative patterns of aqueous solutions of typical simple electrolytes, potassium chloride, sodium chloride, calcium chloride, and lanthanum chloride were observed on a cover glass. The macroscopic broad rings were formed at the outside edge of the drying area, which shrunk from the initial liquid area. The drying area and then the size of the broad ring decreased as salt concentration decreased. The microscopic block-like and dendritic cross-like patterns were formed for all the salts. Size of the single crystals on a cover glass increased sharply as salt concentration increased. This concentration dependency of the crystal size is just opposite to the size change of crystals in bulk solution in the homogeneous nucleation and crystallization mechanism. The drying patterns of the binary mixtures KCl + $CaCl_2$, NaCl + $CaCl_2$, and NaCl + $LaCl_3$ were observed. Size of the broad rings was increased by the mixing. The microscopic structures were, on the other hand, insensitive to the mixing.

Acknowledgments Financial supports from the Ministry of Education, Culture, Sports, Science and Technology, Japan and Japan Society for the Promotion of Science are greatly acknowledged for Grants-in-Aid for Exploratory Research (17655046 to T.O.), Scientific Research on Priority Area (A) (11167241 to T.O.), and Scientific Research (B) (11450367 and 18350057 to T.O. and 19350110 to A.T.), respectively. Catalysts and Chemicals Co. is thanked deeply for his providing the colloidal silica sphere samples used in this work.

References

1. Benard H (1900) Rev Gen Sci Pure Appl 11:1261
2. Benard H (1900) Rev Gen Sci Pure Appl 11:1309
3. Terada T (1928) Rep Aeronaut Res Inst Japan 3:287–326
4. Terada T (1929) Rep Aeronaut Res Inst Japan 4:447–470
5. Nakaya U (1947) Memoirs of Torahiko Terada (in Japanese). Kobunsya, Tokyo
6. Okubo T, Kimura H, Kimura T, Hayakawa F, Shibata T, Kimura K (2005) Colloid Polym Sci 283:1
7. Okubo T (2006) Colloid Polym Sci 285:225
8. Okubo T (2008) Colloid Polym Sci. doi:10.1007/s00396-008-1947-2
9. Okubo T (2008) Colloid Polym Sci. doi:10.1007/s00396-008-1960-5
10. Okubo T, Okamoto J, Tsuchida A (2008) Colloid Polym Sci 286:1123
11. Okubo T (2008) Colloid Polym Sci 286:1307
12. Okubo T (2006) Colloid Polym Sci 284:1191
13. Okubo T (2006) Colloid Polym Sci 284:1395
14. Okubo T, Okamoto J, Tsuchida A (2007) Colloid Polym Sci 285:967
15. Okubo T (2007) Colloid Polym Sci 285:1495
16. Okubo T, Okamoto J, Tsuchida A (2008) Colloid Polym Sci 286:385
17. Okubo T, Okamoto J, Tsuchida A (2008) Colloid Polym Sci 286:941
18. Yamaguchi T, Kimura K, Tsuchida A, Okubo T, Matsumoto M (2005) Colloid Polym Sci 283:1123
19. Okubo T (2006) Colloid Polym Sci 285:331
20. Okubo T (2008) Nanoparticles: syntheses, stabilization, passivation and functionalization. In: Nagarajan R, Hatton TA (eds) ACS Symp Ser 996, Chap 19. ACS, Washington, DC, p 256
21. Vanderhoff JW (1973) J Polym Sci Symp 41:155
22. Palmer HJ (1976) J Fluid Mech 75:487
23. Nicolis G, Prigogine I (1977) Self-organization in non-equilibrium systems. Wiley, New York
24. Anderson DM, Davis SH (1995) Phys Fluids 7:248
25. Ohara PC, Heath JR, Gelbart WM (1997) Angew Chem 109:1120
26. Maenosono S, Dushkin CD, Saita S, Yamaguchi Y (1999) Langmuir 15:957
27. Nikoobakht B, Wang ZL, El-Sayed MA (2000) J Phys Chem 104:8635
28. Ung T, Litz-Marzan LM, Mulvaney P (2001) J Phys Chem B 105:3441
29. Cachile M, Benichou O, Cazabat AM (2002) Langmuir 18:7985
30. Deegan RD, Bakajin O, Dupont TF, Huber G, Nagel SR, Witten TA (1997) Nature 389:827
31. Deegan RD, Bakajin O, Dupont TF, Huber G, Nagel SR, Witten TA (1997) Phys Rev E 62:756
32. Okubo T, Yamada T, Kimura K, Tsuchida A (2005) Colloid Polym Sci 283:1007
33. Okubo T, Okuda S, Kimura H (2002) Colloid Polymer Sci 280:454
34. Okubo T, Kimura K, Kimura H (2002) Colloid Polym Sci 280:1001
35. Okubo T (2008) Colloid Polym Sci 286:1527
36. Kimura K, Kanayama S, Tsuchida A, Okubo T (2005) Colloid Polym Sci 283:898
37. Okubo T, Shinoda C, Kimura K, Tsuchida A (2005) Langmuir 21:9889
38. Okubo T, Onoshima D, Tsuchida A (2007) Colloid Polym Sci 285:999
39. Okubo T, Yamada T, Kimura K, Tsuchida A (2006) Colloid Polym Sci 284:396
40. Okubo T, Itoh E, Tsuchida A, Kokufuta E (2006) Colloid Polym Sci 285:339
41. Okubo T, Nakagawa N, Tsuchida A (2007) Colloid Polym Sci 285:1247
42. Okubo T, Kimura K, Tsuchida A (2008) Colloid Polym Sci 286:621